Thermodynamic and Thermoeconomic Optimization of an Absorption Refrigeration System integrated with Refinery Crude Oil Furnace

Mehdi Tavakoli [1], Seyyed Ehsan Shakib [*2], Majid Amidpour [3], Mohammad Mustafa Ghafurian [4]

[1] MSc Islamic Azad University- Sciences & Research Branch, Hesarak, Tehran, Iran
[2] Assistant Professor Department of Mechanical Engineering, Bozorgmehr University of Qaenat, Qaen, Iran
[3] Professor Faculty of Mechanical Engineering, K.N. Toosi University of Technology, Tehran, Iran
[4] PhD Candidate of Mechanical Engineering, Ferdowsi University of Mashhad, Mashhad, Iran

Abstract: In the present study, exhaust gases from Tehran refinery crude oil furnace are used in a Heat Recovery Steam Generator (HRSG)for generating steam. Then, the steam is directed to a double effect absorption refrigeration cycle to produce cooling. To meet the object, mass and energy balance equations of the coupling is carried out for both the HRSG and the absorption chiller and unknown thermodynamic parameters of the system are evaluated. Afterward, by conducting exergy analysis and using the thermoeconomic method, the cost of the product (refrigeration here) is calculated. Finally, optimization is accomplished simultaneously on both HRSG and absorption chiller in order to minimize the cooling cost by the means of a Genetic algorithm. The outcomes indicate that by using the optimized integrated system 5627 tons of refrigeration is obtainable at the price of 0.0104 (USD per second). Since the flue gas was wasting to environment pricelessly, it should be noted that by implementing the proposed coupling 1.186×10^7 cubic meter of natural gas with the price of 1.508×10^6(USD) will be saved annually.

1. Introduction

Waste heat, in the most general sense, is the energy associated with the waste streams of air, exhaust gases, and/or liquids that leave the boundaries of a plant or building and enter the environment. In a more restricted definition, waste heat is the energy which is rejected from a process at a temperature high enough above the ambient temperature to permit the economic recovery of some fraction of that energy for useful purposes (Doty & Turner, 2004). The strategy of how to recover this heat depends on the temperature of the waste heat and the economics involved (Thumann & Mehta, 2001).

The energy and global warming crises have drawn renewed interests to thermally driven cooling systems from the air conditioning and process cooling facilities. The lithium bromide-water absorption chiller is one of the favorites due to the following specific reasons: (i) it can

be thermally driven by low-temperature heat as well as waste heat, which substantially reduce carbon dioxide emission; (ii) its use of water as a refrigerant; (iii) it is quiet and cheap to maintain, being nearly void of high speed moving parts; (iv) its vacuumed operation renders to scale up applications (Wang & Chua, 2009).

Heat recovery systems in which absorption chillers have been used to produce cooling have been studied by many researchers. Khoshgoftarmanesh and babaelahi have a 160 MW combined cycle power plant from Exergetic, Economic, Environmental aspects simultaneously through Multi-Objective Optimization (Khoshgoftar Manesh & Babaelahi, 2017). Golchoobian et al. studied three combined power and refrigeration cycles for a defined demand and same fuel consumption in a 24 hours period, thermodynamically. Power cycle was used for power generation and also ejector refrigeration

_____
[*] Corresponding Author.
Authors' Email Address: [1] M. Tavakoli (meh.tavakoli@gmail.com), [2] S. E. Shakib (ehshakib@gmail.com), [3] M. Amidpour (amidpour@kntu.ac.ir), [4] M. M. Ghafurian (m.m.ghafoorian@mail.um.ac.ir)

cycle is used to produce cooling (Golchoobian, Amidpour, & Pourali, 2018). Jeong et al. carried out a numerical simulation to predict the transient operating characteristics and performance of an absorption heat pump recovering low- grade waste heat (Jeong, Kang, & Karng, 1998). Ameri and Hejazi presented an overview of an intake air cooling system that uses a steam absorption chiller and an air cooler in order to increase the performance of a gas turbine (Ameri & Hejazi, 2004). Wu and Wang worked on combined cooling, heating and power (CCHP) systems (Wu & Wang, 2006). They studied the various options to produce cooling in CCHP systems including absorption cooling, adsorption cooling, and desiccant dehumidifiers Deng et al. discussed thermally activated cooling technologies for CCHP systems are presented here in detail, mainly including absorption and adsorption refrigeration, and desiccant cooling (Deng, Wang, & Han, 2011).

Absorption refrigeration technology is studied by many researchers. ShariatiNiasar et al. presented a novel mixed fluid cascade natural gas liquefaction process and analyzed it through exergy and exergoeconomic methods. They used a water-ammonia absorption refrigeration cycle instead of one of the vapor compression cycles (Shariati Niasar et al., 2017). Xu et al. carried out a thermodynamic analysis to study the effect of design parameters on the performance of double effect absorption of the series flow type (Xu, Dai, Tou, & Tso, 1996). Arun et al. evaluated the equilibrium temperatures at the low pressure (LP) generator for double effect series flow lithium bromide–water vapor absorption chiller and the system performance at these temperatures (Arun, Maiya, & Murthy, 2000). Chua et al. presented a thermodynamically consistent set of specific enthalpy, entropy, and heat capacity fields for LiBr-water solution (Chua, Toh, Malek, Ng, & Srinivasan, 2000). Srikhirin et al. provided a literature review on absorption refrigeration technology (Srikhirin, Aphornratana, & Chungpaibulpatana, 2001). In 2003, Florides et al. presented a method to evaluate the characteristics and performance of a single stage lithium bromide-water absorption machine (Florides, Kalogirou, Tassou, & Wrobel, 2003). Kilic and Kaynakli performed the first and second law thermodynamic analysis of a single effect absorption refrigeration cycle with LiBr-water as working fluid pair (Kilic & Kaynakli, 2007). Kaushik and Arora presented the energy and exergy of single effect and series flow double effect LiBr-water absorption systems (Kaushik & Arora, 2009). Misra et al. applied the thermoeconomic concept to the optimization of a double effect LiBr-water system, aimed at minimizing its overall product cost (Misra, Sahoo, & Gupta, 2005). They used a simplified cost minimization methodology based on the thermoeconomic concept to carry out the costs of all the internal flows and products of the system by formulating thermoeconomic cost balances. Bereche et al. carried out a thermoeconomic analysis of single effect and double effect LiBr-water absorption refrigeration system in which the methodology of functional analysis with negentropy is used (Bereche, Palomino, & Nebra, 2009).

The energy of absorption refrigeration systems is usually supplied from waste heat sources although some researchers recently studied the integration of solar energy and absorption chillers.

Winston et al. have built a solar thermal cooling system using non-tracking External Compound Parabolic Concentrators for cooling seasons (Winston, Jiang, & Widyolar, 2014). The solar cooling is used to power a 23 kW double effect (LiBr) absorption chiller. Lu and Wang presented experimental performance investigation and economic analysis of three small solar cooling systems with these different kinds of collectors and chillers (Lu & Wang, 2014). Jayasekara and Halgamuge studied a combined effect absorption cycle that can utilize two energy sources at different temperature ranges or a single source at a wide temperature range (Jayasekara & Halgamuge, 2014).

In the present study, the hot flue gas from the furnace exhaust is used to generate steam in a Heat Recovery Steam Generator (HRSG). Then the produced steam is sent to a double effect absorption chiller in order to produce chilled water. The cost of produced cooling is evaluated by using thermoeconomic (exergoeconomic) method. In other words, the cost of the main product, the cooling cost, was calculated as a function of the exergy of the heat source. Finally, optimization is accomplished on the system by considering most of the operating parameters. The decision variables in optimization are chosen from both HRSG and the Chiller. It is the first study in which the HRSG and Double Effect Absorption Chiller is optimized simultaneously as an integrated system.

2. System Modeling

2.1. HRSG Modeling

Heat recovery steam generator (HRSG) is applied for recovering the heat potential of high-temperature flue gas to produce the required steam of utilities. Physical properties and mole fraction of the flue gas are shown in Table 1.

Table 1. physical properties and mole fractions of furnace flue gas

property	amount
Temperature	460(°C)
pressure	101.3 (kpa)
mass flow rate	162100 (kg/hr)=45(kg/s)
Mole fraction of CO_2	0.052749
Mole fraction of H_2O	0.105596
Mole fraction of O_2	0.093324
Mole fraction of N_2	0.748286

The principles of heat recovery steam generators are investigated by many researchers. A comprehensive study is accomplished by reference (Ganapathy, 2003) in which methods for design, applications, and calculations of these heat exchangers are discussed. Hot flue gas condition and temperature have sensible effects on configuration of the HRSG. In this study, a single-pressure water tube boiler is chosen. The device includes three main sections: (1) economizer (2) evaporator (3) super heater. This model generates single pressure steam at the exit of the super heater section that its schematic configuration is shown in Fig. 1.

In this model, hot flue gas enters the super heater at the temperature of T_{g1} and leaves the economizer at the temperature of T_{g4}. On the water/steam side, cool water enters the economizer at the temperature and the enthalpy of T_1, h_1 respectively and super-heated steam leaves the super heater at the temperature and enthalpy of T_6, h_6 respectively. Energy balance equations in different parts of the HRSG can be written as follows:

$$\dot{m}_g c_p (T_{g4} - T_{g3}) + \dot{m}_s (h_2 - h_1) = 0 \qquad (1)$$

$$\dot{m}_g c_p (T_{g3} - T_{g2}) + \dot{m}_s (h_4 - h_3) = 0 \qquad (2)$$

$$\dot{m}_g c_p (T_{g2} - T_{g1}) + \dot{m}_s (h_6 - h_5) = 0 \qquad (3)$$

In these equations, T_{g1}, T_{g2}, T_{g3}, and T_{g4} are the hot gas temperature in different parts of HRSG and h_1, h_2... h_6 are enthalpies of water or steam inside the heat exchanger tubes.
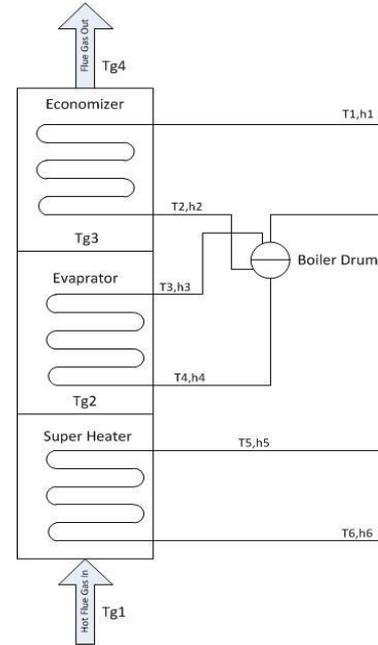

Figure 1. The schematic of the model of the HRSG

2.1.1. Pinch and approach temperatures

As it is shown in Fig. 2 the pinch point is the temperature difference between the saturation temperature and the HRSG evaporator enter temperature. It is desirable to make the pinch point as small as possible without making the cost of the HRSG astronomical.
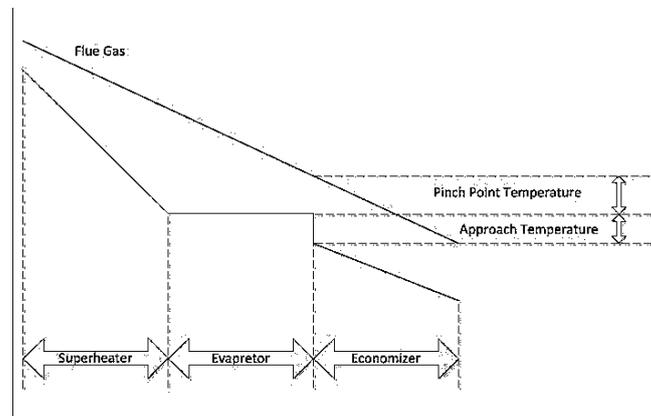

Figure 2. pinch and approach points temperature

The approach point temperature is the difference between the economizer water outlet temperature and the Saturation temperature of the steam. This temperature will guarantee that no steaming will occur in the economizer section.

For solving energy balance equations (equations 1 to 3), the following assumptions are considered:

- The Pinch point temperature is 15 ˚C
- The Approach point temperature is 15 ˚C
- Water/Steam line pressure in HRSG is 10 bar
- Specific Heat Capacity of the flue gas is constant and equal to 1.2 kJ/kg.K
- The feed water temperature is 25 ˚C
- The temperature of produced steam in super heater is 450 ˚C
- Dew point temperature of the flue gas is 130 ˚C

It should be noted that among proposed assumptions, there are the decision variables of the optimization process which presented in the next parts.

2.2. Double Effect Absorption Chiller

As shown in Fig. 3, a double effect absorption chiller consists of two generators, two solution heat exchangers, an evaporator, a condenser, and an absorber.

High- temperature heat is supplied at High Pressure Generator (HPG) and the generated vapor in this section is used as a heat source at Low Pressure Generator (LPG), in which additional vapor is generated.

In a double-effect absorption chiller, the entire vapor generated at the HPG is fully condensed at the low- pressure LPG(Arun et al., 2000). It involves three pressure levels, i.e. high, medium and low. The HPG functions at high pressure and temperature, the LPG and condenser operate at medium pressure, and the evaporator and the absorber work at a low-pressure level. The weak solution leaving the absorber is pumped to the high- temperature generator through solution heat exchangers (HX1 and HX2). A high- temperature heat source adds heat to HPG to generate water vapor from a weak solution. The strong solution leaving the HPG enters to the LPG where the refrigerant (water) vapor coming from HPG is condensed due to the low temperature of the strong solution. Latent heat of the vapor is utilized in generating water vapor from the strong solution. The strong solution, therefore, becomes stronger (in Lithium-Bromide) and it is delivered to the absorber through the solution heat exchanger 2 (HX2). Thus in a double effect system, the second effect generator increases the quantity of water vapor generated for the same amount of heat input. This results in higher values of COP than those achieved in the single effect system(Kaushik & Arora, 2009).
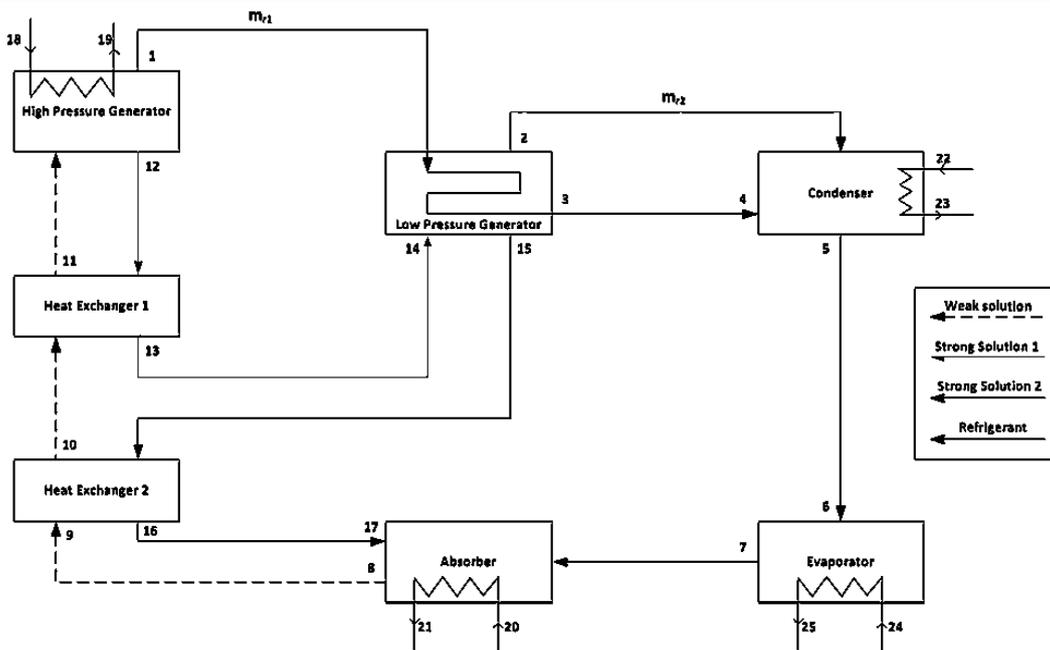

Figure 3. schematic diagram of absorption cooling cycle

2.2.1. Mass and Energy Balance Equations

The energy analysis of absorption systems involves the application of principles of mass conservation, species conservation and the first law of thermodynamics. The general equations are given in - Table 2.

Table 2. Mass and energy balance equations (Bereche et al., 2009; Florides et al., 2003; Kaushik & Arora, 2009; Kilic & Kaynakli, 2007; Misra et al., 2005; Srikhirin et al., 2001)

Mass balance equations	Number
$m_{ss1} = m_{ws} - m_{r1}$	**(4)**
$m_{ws}x_{ws} = m_{ss1}x_{ss1}$	**(5)**
$m_{ss2} = m_{ws} - m_r$	**(6)**
$m_{ss1}x_{ss1} = m_{ss2}x_{ss2}$	**(7)**
$m_r = m_{r1} + m_{r2}$	**(8)**
energy balance equations	
$Q_{HPG} + m_{ws}h_{11} - m_{r1}h_1 - m_{ss1}h_{12} = 0$	**(9)**
$m_{ss1}h_{14} + m_{r1}h_1 - m_{ss2}h_{15} - m_{r1}h_3 - m_{r2}h_2 = 0$	**(10)**
$m_{r2}h_2 + m_{r1}h_4 - Q_{condenser} - (m_{r1} + m_{r2})h_5 = 0$	**(11)**
$(m_{r1} + m_{r2})h_6 + Q_{evaporator} - (m_{r1} + m_{r2})h_7 = 0$	**(12)**
$(m_{r1} + m_{r2})h_7 + m_{ss2}h_{17} - m_{ws}h_8 - Q_{absorber} = 0$	**(13)**
$m_{ss2}\eta_{HX2}(h_{15} - h_{16}) - m_{ws}(h_{10} - h_9) = 0$	**(14)**
$m_{ss1}\eta_{HX1}(h_{12} - h_{13}) - m_{ws}(h_{11} - h_{10}) = 0$	**(15)**
$E_{HX2} = \dfrac{T_{15} - T_{16}}{T_{15} - T_9}$	**(16)**
$E_{HX1} = \dfrac{T_{12} - T_{13}}{T_{12} - T_{11}}$	**(17)**

In the above table, ss, ws, r, HPG, and HX reference to a strong solution, weak solution, refrigerant, high- pressure generator, and heat exchanger. The following assumptions are considered for solving eq.1 to 14 (Xu & Dai, 1997):

➢ The pressure drop and heat loss in pipes and components are negligible.
➢ The high- pressure level (including HPG) is 0.93 bars.
➢ The medium pressure level (including LPG and condenser) is 0.0779 bars.
➢ The low- pressure level (including evaporator and absorber) is 0.0087 bars.
➢ The temperature of HPG is 153˚C.
➢ The pinch point temperature in LPG is 15˚C.
➢ The temperatures of condenser, evaporator, and absorber are 41˚C, 5˚C, and 38.4˚C respectively.
➢ The effectiveness of the first and second heat exchangers is 0.7.

Many of the assumptions made above are involved in decision variables and at the end of optimization; the optimal values will be carried

out and replaced with them. Having used these assumptions, enthalpy and entropy of the streams are calculated. For calculating enthalpy and entropy of the solution, data is taken from ref. (Chua et al., 2000)and for pure refrigerant streams is taken from water and steam standard tables.

By using these assumptions, there are 14 unknown parameters in mass and energy balance equations and heat exchangers effectiveness equations. The unknown parameters of equations (4) to (17) are as follows:

1. Mass flow rate of weak solution leaving the absorber: m_{ws}
2. Mass flow rate of refrigerant vapor leaving the HPG: m_{r1}
3. Mass flow rate of refrigerant vapor leaving the LPG: m_{r2}
4. Mass flow rate of refrigerant stream entering the evaporator: m_r
5. Mass flow rate of strong solution stream leaving the HPG: m_{ss1}
6. Mass flow rate of strong solution stream leaving the LPG: m_{ss2}
7. Solution concentration of strong solution leaving the HPG: x_{ss1}
8. Temperature of weak solution stream leaving HX2: T_{10}
9. Temperature of weak solution stream leaving HX1: T_{11}
10. Temperature of strong solution stream leaving HX1: T_{13}
11. Temperature of strong solution stream leaving HX2: T_{16}
12. Heat transfer rate in condenser: $Q_{condenser}$
13. Heat transfer rate in evaporator: $Q_{evaporator}$
14. Heat transfer rate in absorber: $Q_{absorber}$

2.3. Heat Exchangers Sizing

In single-pass heat exchangers, the temperature difference (ΔT) between hot and cold fluids varies along with the heat exchanger. Hence, it is convenient to use a mean temperature (ΔT$_m$) between hot and cold fluids. So the total heat transfer rate (Q̇) between the fluids can be determined from the following equation:

$$\dot{Q} = AU\Delta T_m \qquad (18)$$

Where, A (m²) is the total heat transfer area and U (W/m2-°C) is the average overall heat transfer coefficient, based on that area. For Equation (22), ΔT$_m$ can be calculated as follows:

$$\Delta T_m = \Delta T_{ln} = \frac{\Delta T_0 - \Delta T_L}{\ln(\Delta T_0 / \Delta T_L)} \qquad (19)$$

Also for equation (22) the overall heat transfer coefficient (U) is defined as(Ozisik, 1985):

$$U = \frac{1}{(D_o/D_i)(1/h_i) + (D_o/D_i)F_i + [1/(2k)D_o \ln(D_o/D_i) + F_o + 1/h_o} \qquad (20)$$

Where D_i and D_o are the inside and the outside diameters of the tubes, h_i and h_o are the heat transfer coefficient inside and outside the tubes, F_i, F_o are the fouling factors of the tubes and k is the thermal conductivity of the material of the tubes. The method of calculating h_i and h_o could be found in Appendix I.

3. Exergy and Thermodynamic Analysis

3.1 Exergy Analysis

Eq. (21) is used to evaluate the physical exergy of different streams in the system.

$$\dot{E} = \dot{m}[h - h_0 - T_0(s - s_0)] \qquad (21)$$

Where $\dot{m}$ is the mass flow rate of the stream, h and s is the enthalpy and entropy of the stream per kg, T_0 is the environmental temperature and h_0 and s_0 are the enthalpy and entropy values of the fluid at the environmental temperature T_0 respectively (Bejan, Tsatsaronis, Moran, & Moran, 1996). The rate of exergy for each stream is calculated while the environment temperature and pressure are assumed as 25°C and 1 bar respectively.
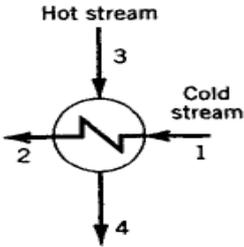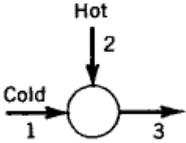
Considering the fuel and product principles in each component, the exergy destruction and exergy efficiency in each component of HRSG and absorption chiller are calculated as follows (Bejan et al., 1996):

$$\dot{E}_D = \sum \dot{E}_F - \sum \dot{E}_P \qquad (22)$$

$$\varepsilon = \frac{\sum \dot{E}_P}{\sum \dot{E}_F} \qquad (23)$$

In order to calculate the exergy efficiency as well as the exergy destruction for each component, it is necessary to first identify the fuel and product. For this purpose, the basic relations of the understudy component is presented in Table 3.

Table 3. The definition of fuel and product exergy for different component of the under study system

component	Schematic figure	Exergy rate of product	Exergy rate of fuel
¹Heat exchanger		$\dot{E}_2 - \dot{E}_1$	$\dot{E}_3 - \dot{E}_4$
Mixing chamber		$\dot{E}_3$	$\dot{E}_1 + \dot{E}_2$
Boiler		$(\dot{E}_6 - \dot{E}_5) + (\dot{E}_8 - \dot{E}_7)$	$(\dot{E}_1 + \dot{E}_2) - (\dot{E}_3 + \dot{E}_4)$
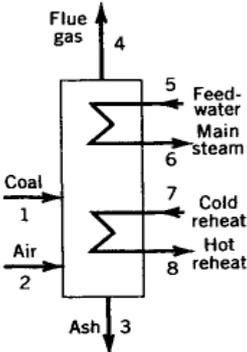
3.2. Thermoeconomic Analysis

The Thermoeconomic analysis is applied to calculate the expenditure cost and the system product cost. Thermoeconomic analysis requires solving energy, exergy, and cost balance equations of the considered HRSG as well as the components of the absorption chiller. The governing equation of thermoeconomic model for the cost balancing of an energy system is written as:

$$C_F + Z = C_P \tag{24}$$

By defining exergy cost of each stream, c, Eq. (37) could be changed to

$$c_F E_F + Z = c_P E_P \tag{25}$$

The above relations are global cost balance equation, which should be applied for a different component. Here, for each component of the combined system, the cost balance equation is taken into account as presented in Table 4.

For solving equations (26) to (33), the auxiliary equations (equations (34) to (46)) have been used according to the principles of thermoeconomic analysis.

4. Optimization Approach

In order to achieve the optimal parameters, an optimization algorithm tool can be used. Although gradient descent methods are the most elegant and precise numerical methods to solve optimization problems, however, they have the possibility of being trapped at local optimum depending on the initial guess of solution. In order to achieve a good result, these methods require very good initial guesses for parameters. Stochastic optimization method such as genetic algorithm (GA) that has been applied for this study seems to be a promising alternative for solving this problem. In general, it is robust search and optimization techniques, able to cope with ill-defined problem domain such as multimodality, discontinuity, and time-variance. GA is a population-based optimization technique that searches the best solution for a given problem based on the concepts of natural selection, genetics, and evolution(Holland, 1992).

Table 4. the thermoeconomic equations of the system

equation	equipment	No.
$c_{g1}\dot{E}_{g1} + c_{1-HRSG}\dot{E}_{1-HRSG} + Z_{CI-HRSG} - c_{g4}\dot{E}_{g4} - c_{18}\dot{E}_{6-HRSG} = 0$	HRSG	(26)
$c_{18}\dot{E}_{18} + c_{11}\dot{E}_{11} + Z_{CI-HPG} - c_1\dot{E}_1 - c_{12}\dot{E}_{12} = 0$	HPG	(27)
$c_1\dot{E}_1 + c_{14}\dot{E}_{14} + Z_{CI-LPG} - c_2\dot{E}_2 - c_3\dot{E}_3 - c_{15}\dot{E}_{15} = 0$	LPG	(28)
$c_2\dot{E}_2 + c_4\dot{E}_4 + Z_{CI-condenser} - c_3\dot{E}_3 - c_5\dot{E}_5 - \Delta C_{condenser} = 0$	Condenser	(29)
$c_6\dot{E}_6 + Z_{CI-evaporator} - c_7\dot{E}_7 - \Delta C_{evaporator} = 0$	Evaporator	(30)
$c_{17}\dot{E}_{17} + c_7\dot{E}_7 + Z_{CI-absorber} - c_8\dot{E}_8 - \Delta C_{absorber} = 0$	Absorber	(31)
$c_9\dot{E}_9 + c_{15}\dot{E}_{15} + Z_{CI-HX2} - c_{10}\dot{E}_{10} - c_{16}\dot{E}_{16} = 0$	Heat Exchanger 1	(32)
$c_{10}\dot{E}_{10} + c_{12}\dot{E}_{12} + Z_{CI-HX1} - c_{11}\dot{E}_{11} - c_{13}\dot{E}_{13} = 0$	Heat Exchanger 2	(33)
$\dfrac{c_1\dot{E}_1 - c_{11}\dot{E}_{11}}{\dot{E}_1 - \dot{E}_{11}} - \dfrac{c_{12}\dot{E}_{12} - c_{11}\dot{E}_{11}}{\dot{E}_{12} - \dot{E}_{11}} = 0$		(34)
$c_{18} - c_{19} = 0$		(35)
$\dfrac{c_2\dot{E}_2 - c_{11}\dot{E}_{14}}{\dot{E}_2 - \dot{E}_{14}} - \dfrac{c_{15}\dot{E}_{15} - c_{14}\dot{E}_{14}}{\dot{E}_{15} - \dot{E}_{14}} = 0$		(36)
$c_1 - c_3 = 0$		(37)
$\dfrac{c_2\dot{E}_2 + c_4\dot{E}_4}{\dot{E}_2 + \dot{E}_4} - \dfrac{c_5\dot{E}_5}{\dot{E}_5} = 0$		(38)
$c_6 - c_7 = 0$		(39)
$\dfrac{c_7\dot{E}_7 + c_{17}\dot{E}_{17}}{\dot{E}_7 + \dot{E}_{17}} - \dfrac{c_8\dot{E}_8}{\dot{E}_8} = 0$		(40)
$c_{12} - c_{13} = 0$		(41)
$c_{15} - c_{16} = 0$		(42)
$c_3 = c_4$		(43)
$c_5 = c_6$		(44)
$c_{16} = c_{17}$		(45)
$c_{13} = c_{14}$		(46)

4.1. Decision Variables

In thermal system design and optimization, it is convenient to identify two types of independent variables. These variables are decision variables and parameters. The decision variables may be varied in the optimization process. However, the parameters remain fixed in a given application. All other variables are dependent variables. Their values are calculated from independent variables using thermodynamic relations.

➢ The selected decision variables in this work are:

➢ Steam pressure (generated by HRSG): $5 \leq P_{Water/Steam} \leq\leq 15\ bar$

➢ Steam temperature: $200 \leq T_{Water/Steam} \leq 500\ ℃$

➢ Pinch point temperature in HRSG: $5 \leq T_{PP} \leq 50\ ℃$

➢ HPG temperature: $100 \leq T_{HPG} \leq 180\ ℃$

➢ HPG pressure: $0.9 \leq P_{HPG} \leq 1.1\ bar$

➢ Condenser temperature: $35 \leq T_{Condenser} \leq 45\ ℃$

➢ Absorber temperature: $33 \leq T_{Absorber} \leq 44$

➢ Absorber inlet cooling water: $28 \leq T_{20} \leq 40\ ℃$

➢ Condenser inlet cooling water: $32 \leq T_{22} \leq 42\ ℃$

➢ Weak solution concentration: $55 \leq x_{ws} \leq 60\ \%$

➢ Strong solution concentration: $60 \leq x_{ss2} \leq 65\ \%$

5. Results and Discussion

The results of the thermodynamic simulation are shown in tables 5 and 6. Table 5 shows the thermodynamic properties of streams of chiller and Table 6 shows heat transfer rates of the components.

Table 5. Thermodynamic properties of chiller streams

Current No.	mass flow rate (kg/s)	temperature (˚C)	pressure (bars)	concentration (percent)	enthalpy (kJ/kg)	entropy (kJ/kg.K)
1	3.73	153	0.93	0	2671	7.3832
2	3.59	82.6	0.0779	0	2654	8.4740
3	3.73	97.6	0.93	0	409	1.2797
4	3.73	97.6	0.93	0	409	0.5858
5	7.32	41	0.0779	0	172	0.5858
6	7.32	5	0.0087	0	21	0.0763
7	7.32	5	0.0087	0	2510	9.0249
8	87.86	38.4	0.0087	57.75	102	0.2171
9	87.86	38.4	0.93	57.75	102	0.2171
10	87.86	54.62	0.93	57.75	154	0.3770
11	87.86	121.67	0.93	57.75	267	0.6886
12	84.13	153	0.93	60.31	335	0.8082
13	84.13	91.14	0.93	60.31	215	0.5026
14	84.13	91.14	0.93	60.31	215	0.5026
15	80.54	82.6	0.0779	63	211	0.4378
16	80.54	51.65	0.0779	63	154	0.2722
17	80.54	51.65	0.0779	63	154	0.2722
18	5.48	450	10	0	3371	0.6198
19	5.48	168	10	0	710	2.0219
20	1380	32	1	0	134	0.4642
21	1380	35.8	1	0	150	0.5160
22	1380	35.8	1	0	150	0.5160
23	1380	37.51	1	0	156.61	0.5391
24	868	12	1	0	50	0.1806
25	868	7	1	0	29	0.1064

Table 6. Temperature, pressure and heat transfer load in each component

Component	Temperature	Pressure	Heat transfer rate (kJ)
HPG	153	0.93	14603
LPG	93	0.0779	---
Condenser	41	0.0779	9803
Evaporator	5	0.0087	18225
Absorber	38.4	0.0087	21921

As can be seen in the table, the cooling capacity of the refrigeration cycle (attainable cooling in the evaporator) is 18225 kW (5182 tons of refrigeration). The Coefficient of Performance (COP) of the chiller which is defined as the ratio of cooling capacity to the heat input the HPG can be calculated as follows:

$$COP = \frac{Q_{evaporator}}{Q_{HPG}} = \frac{18225}{14603} = 1.25$$

Table 7 shows the results of solving heat exchangers sizing for HRSG and the absorption chiller components. According to the table, overall exergy destruction rate before the optimization is 11089 kJ/s and highest exergy efficiency (88.78%) is related to LPG.

By using heat transfer surface areas, the weight of heat exchangers of HRSG and chiller are calculated and the prices are evaluated as shown in Table 9.

Table 7. Heat exchangers calculations results

Component	LMTD (°C)	Overall heat transfer coefficient (W/(m².K))	Heat transfer rate (kW)	Required heat transfer area (m²)
HRSG				
economizer	61.48	86	3249	515
Evaporator	76.27	93	11056	1562
Super heater	67.88	99	3260	487
Double effect absorption chiller				
Absorber	4.21	2912	21921	1784
HX1	28.85	478	10004	439
HPG	94.45	2702	14602	57
HX2	15.49	705	4796	705
LPG	35.83	2568	8440	91
Condenser	4.28	3473	9803	658
Evaporator	3.99	1803	18224	2533

Table 8. exergy destruction rate and exergy efficiency in each component

Component	Exergy destruction rate (kJ/s)	Exergy efficiency (ε)
Heat Recovery Steam Generator		
Economizer	487	55
Evaporator	1465	72
Super heater	326	82.75
Double Effect Absorption Chiller		
HPG	1276	88.5
LPG	185	88.78
Condenser	1082	20.38
Evaporator	310	76.1
Absorber	750	46.3
Solution heat exchanger 1	4184	78.7
Solution heat exchanger 2	1022	65.77

Table 9. price estimation and overall implementation expenditure of the chiller

Component	Heat transfer area (m²)	Price (USD)
Double effect absorption chiller		
Absorber	1784	1349246
HX1	439	609864
HPG	57	27307
HX2	705	593346
LPG	91	43781
Condenser	658	520191
Evaporator	2533	1915245

The optimal values of decision variables, decision variables and thermoeconomic parameter values for the base case and optimal solution of GA are presented in Table 10.

The result indicates that by increasing the Pinch Point temperature and the steam pressure, the heat transfer area of HRSG will be decreased. Moreover, the mass flow rate of generated steam in the super heater is increased by producing steam with lower temperature in higher pressure than initial pressure.

According to the obtained results, the optimized values of temperatures of HPG and LPG are lower than the initial system, while the pressures of these components are higher after optimization. In general, it is obtainable that the optimized system works under lower temperature in comparison with the initial system.

With optimized decision variables, the COP of the absorption chiller is 1.45, the steam flow rate of HRSG is 6.87 kg/s, total heat transfer area is 7140 m² for a capacity of 19790 kW of refrigeration. The changes in heat transfer areas are shown in fig. 2.

As can be seen in Fig. 4, in some components heat transfer area is increased by optimization, however, the total heat transfer area is reduced after optimization.

Generally, changes in the main parameters of the system can be summarised as follows:

√ Cooling capacity of the system is increased from 18225 kW to 19790 kW by 8.5%.

√ The COP of the system is changed by 16.9%. While the COP of initial system is 1.24, the COP of optimized system is 1.45.

√ Exergy destruction rate is decreased by 33% after optimization.

√ Due to optimization, total heat transfer area is decreased by 22.5%, from 9219 m² to 7140 m².

√ After optimization, capital investment of the proposed coupling is reduced by 555840 (USD).

√ The price of the produced cooling is decreased by 7%. It decreased from 1.98×10^{-6} (Dollar per second) to 1.84×10^{-6} (Dollar per second).

Table 10. values of object function, decision variables and thermoeconomic parameter for base case and optimal solution

Parameters	Unit	Base case	Optimal
Objective function			
Total product cost	$/TR	0.0190	0.0171
Decision variables			
$P_{Water/Steam}$	Bar	10	5.97
$T_{Water/Steam}$	°C	450	230.43
T_{PP}	°C	15	35.87
T_{HPG}	°C	153	151.02
P_{HPG}	Bar	0.93	1.10
$T_{Condenser}$	°C	41	37.21
$T_{Absorber}$	°C	38.4	35.95
T_{22}	°C	32	31.82
T_{20}	°C	35.8	34.23
X_{ws}	%	57.75	55
X_{ss2}	%	63	64.95
HRSG thermodynamic parameters			
T_{g4}	°C	134.87	135.57
m_s	kg/s	5.48	6.38
Chiller thermodynamic parameters			
m_{r1}	kg/s	3.73	4.27
m_{r2}	kg/s	3.59	3.56
m_r	kg/s	7.32	7.82
m_{ss1}	kg/s	60.31	60.01
m_{ss2}	kg/s	80.54	43.26
m_{ws}	kg/s	87.86	51.696
High pressure	Bar	0.93	1.09
Medium pressure	Bar	0.0779	0.0636
Low pressure	Bar	0.0087	0.0087

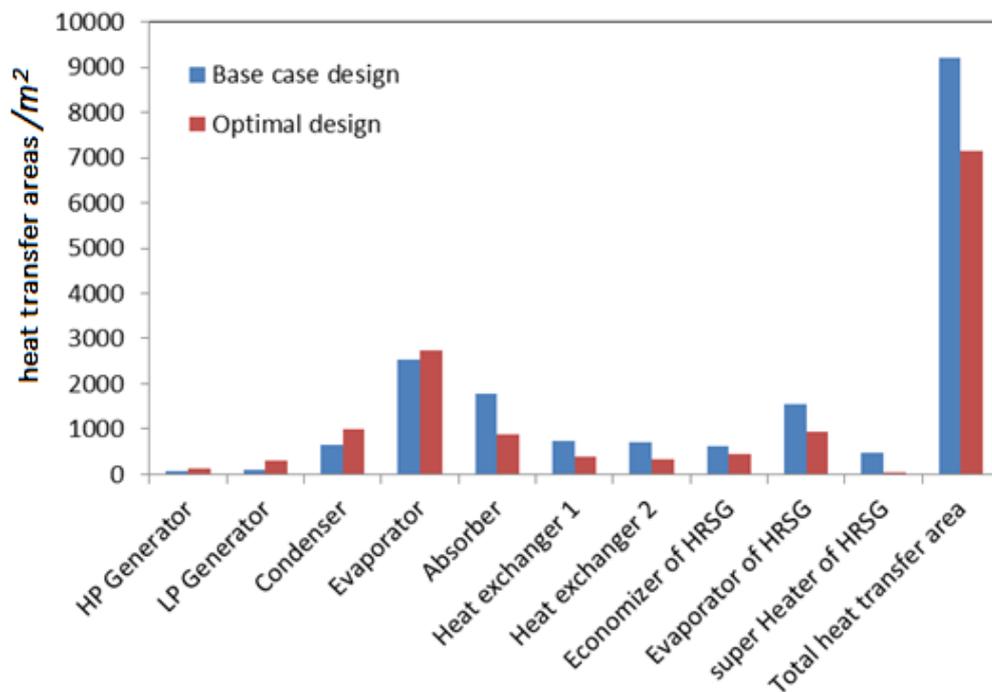| Parameters	Unit	Base case	Optimal
Heat transfer rates in chiller components			
HPG	kW	14603	14131
Condenser	kW	9803	10094
Evaporator	kW	18225	19486
Absorber	kW	21921	22468
Other parameters			
COP	---	1.25	1.38
Capital investment of HRSG	$	1,326,833	1,003,605
Capital investment of Chiller	$	5,058,984	5,897,359

Figure 5. comparison of heat transfer areas of the components before and after the optimization

6. Conclusion

In this paper, a combined system consisting of a double effect absorption chiller and an HRSG was coupled with a refinery furnace located in Tehran to provide chilled water from furnace exhaust gasses. At first, thermodynamic analysis was conducted to the system to calculate unknown thermodynamic parameters like mass flow rates and heat loads of heat exchangers. Afterward, by calculating heat transfer areas of the components and exergy of the streams and using Thermoeconomic approach, the price of the product (refrigeration) was calculated. Finally, the system was optimized by the means of the Genetic Algorithm (GA). The optimal solution of GA proposed a system with the lowest price of the product and the highest cooling capacity as well.

In fact, in comparison with the base case of HRSG and Absorption chiller, the optimal

solution showed 33% increase in exergy efficiency and 7% decrease in the total cost of products. Moreover, compared with the base case, the optimal solution presented a system with lower heat transfer areas and therefore, lower total capital investment is needed. It is obtainable that thermoeconomic analysis of a system is able to provide suggestions about potential cost-effective improvements achievable by the means of changes in the values of the internal operating parameters of the system.

The annual cost of producing 5672 tons of refrigeration is 3.28×10^5 (USD). To produce the same amount of cooling with natural gas, 1.186×10^7 cubic meter of natural gas with the price of 1.508×10^6 (USD) is needed. Consequently, by using the integrated system, the price of the product is one-fifth to produce cooling with natural gas. Besides, the use of waste heat in this plan has many

environmental advantages that conserving natural resources can be considered as one of them.

Appendix I

For calculating h_i, there are other factors that initially need to be evaluated:

$$Re_i = \frac{4 * m_s}{\pi * D_i * \mu} \qquad (A1)$$

$$Pr_i = \frac{\mu * c_p}{k} \qquad (A2)$$

$$Nu_i = \frac{(f/8) * Re * Pr}{K_1 + K_2(f/8)^{1/2} * (Pr^{2/3} - 1)} \qquad (A3)$$

Where, $f = (1.821 * log_{10}^{Re} - 1.64)^{-2}$, $K_1 = 1 + 3.4f$ and $K_2 = 11.7 + (1.8/Pr^{1/3})$. Accordingly h_i can be calculated as follows:

$$h_i = \frac{Nu_i * k}{D_i} \qquad (A4)$$

Where, Nu is Nusselt Number and k is thermal conductivity of fluid.

Equations for calculating h_o in HRSG are as follows (Ganapathy, 2003):

$$h_o = 0.9 * G^{0.6} \frac{F}{d^{0.4}} \qquad (A5)$$

Where G is Gas mass velocity (lb/ft² h).

$$F = k^{0.67} \frac{C_p^{0.33}}{\mu^{0.27}} \qquad (A6)$$

k is gas thermal conductivity and the factor F has been computed for air and flue gases, and a good estimate is given in Table (5)(Winston et al., 2014).

Table A1. F Factor for air and flue gases

Temperature (°C)	F
93	0.094
204	0.103
315	0.110
426	0.116
537	0.123
648	0.130

The gas mass velocity G is given by

$$G = 12 * \frac{W_g}{N_w L(S_T - d)} \qquad (A7)$$

For Absorption chiller, the overall heat transfer in each component is given by equation 18. For this equation, the values of fouling factors (f_i, f_o) are considered as negligible. The thermal conductivity of copper tubes is calculated from the following equation:

$$K_{copper} = 4.583333E^{-09}T^4 - 2.916667E^{-4}T^2 - 0.1108333T + 386 \qquad (W/mK) \qquad (A8)$$

Where, T is the temperature of the component.

The following equation is recommended in the case of condensation on a single horizontal tube which gives the average heat transfer coefficient (Florides et al., 2003):

$$h_m = 0.725 \left[\frac{g\rho_l(\rho_l - \rho_v)h_{fg}k_l^3}{\mu_l(T_v - T_w)D_o} \right]^{0.25} \qquad (A9)$$

Where k_l is the thermal conductivity of liquid (W/m K). For determining an overall heat transfer coefficient (U), physical properties in equation (A8) need to be calculated at the mean wall surface and vapor saturation temperature.

Nomenclature

A	Area(m²)
C	Cost ($/kJ)
c	Cost ($/sec)
CCHP	combined cooling, heating and power
COP	Performance operation coefficient (%)
E	Exergy (kW)
e	Exergy(kJ/kg)
h	Enthalpy(kJ/kg)
HRSG	Heat recovery steam generator
HPG	High pressure generator
LPG	Low pressure generator
m	Flow rate (kg/s)
P	Pressure (bar)
Q	Heat (kW)
S	Entropy (kJ/kg.K)
T	Temperature (°C)
U	Average overall transfer coefficient (W/m2.°C)
X	Mass fraction
Z	Equipment cost ($/sec)

Subscript

D	distraction
p	product
f	fuel
g	gas
Hx	Heat exchanger
r	Refrigerator
ss	Strong solution
ws	Weak solution

Greek symbols

ε	Exergy Efficiency (%)
Δ	Different
η	Efficiency (%)

References

Ameri, M., & Hejazi, S. (2004). The study of capacity enhancement of the Chabahar gas turbine installation using an absorption chiller. *Applied thermal engineering, 24*(1), 59-68.

Arun, M., Maiya, M., & Murthy, S. S. (2000). Equilibrium low pressure generator temperatures for double-effect series flow absorption refrigeration systems. *Applied thermal engineering, 20*(3), 227-242.

Bejan, A., Tsatsaronis, G., Moran, M., & Moran, M. J. (1996). *Thermal design and optimization*: John Wiley & Sons.

Bereche, R. P., Palomino, R. G., & Nebra, S. (2009). Thermoeconomic analysis of a single and double-effect LiBr/H2O absorption refrigeration system. *Int. J. Thermodyn, 12*(2), 89-96.

Chua, H., Toh, H., Malek, A., Ng, K., & Srinivasan, K. (2000). Improved thermodynamic property fields of LiBr–H2O solution. *International Journal of Refrigeration, 23*(6), 412-429.

Deng, J., Wang, R., & Han, G. (2011). A review of thermally activated cooling technologies for combined cooling, heating and power systems. *progress in energy and combustion science, 37*(2), 172-203.

Doty, S., & Turner, W. C. (2004). *Energy management handbook*: Crc Press.

Florides, G. A., Kalogirou, S. A., Tassou, S. A., & Wrobel, L. (2003). Design and construction of a LiBr–water absorption machine. *Energy conversion and management, 44*(15), 2483-2508.

Ganapathy, V. (2003). Industrial boilers and heat recovery steam generators.

Golchoobian, H., Amidpour, M., & Pourali, O. (2018). Thermodynamic analysis of three combined power and refrigeration Systems based on a demand. *Gas Processing Journal 6(1), 29-40.*

Holland, J. H. (1992). *Adaptation in natural and artificial systems: an introductory analysis with applications to biology, control, and artificial intelligence*: MIT press.

Jayasekara, S., & Halgamuge, S. K. (2014). A combined effect absorption chiller for enhanced performance of combined cooling heating and power systems. *Applied energy, 127*, 239-248.

Jeong, S., Kang, B., & Karng, S. (1998). Dynamic simulation of an absorption heat pump for recovering low grade waste heat. *Applied thermal engineering, 18*(1-2), 1-12.

Kaushik, S., & Arora, A. (2009). Energy and exergy analysis of single effect and series flow double effect water–lithium bromide absorption refrigeration systems. *International Journal of Refrigeration, 32*(6), 1247-1258.

Khoshgoftar Manesh, M. H., & Babaelahi, M. (2017). Thermoeconomic And Environmental Optimization Of A 160 Mw Combined Cycle Power Plant By Moea. *Gas Processing Journal* 5(2), 79-96.

Kilic, M., & Kaynakli, O. (2007). Second law-based thermodynamic analysis of water-lithium bromide absorption refrigeration system. *Energy, 32*(8), 1505-1512.

Lu, Z., & Wang, R. (2014). Experimental performance investigation of small solar air-conditioning systems with different kinds of collectors and chillers. *Solar Energy, 110*, 7-14.

Misra, R., Sahoo, P., & Gupta, A. (2005). Thermoeconomic evaluation and optimization of a double-effect H2O/LiBr vapour-absorption refrigeration system. *International Journal of Refrigeration, 28*(3), 331-343.

Ozisik, M. N. (1985). Heat transfer: a basic approach.

Shariati Niasar, M., Amidpour, M., Ghorbani, B., Rahimi, M.-J., Mehrpooya, M., & Hamedi, M.-H. (2017). Superstructure of Cogeneration of Power, Heating, Cooling and Liquid Fuels Using Gasification of Feedstock with Primary Material of Coal for Employing in LNG Process. *Gas Processing Journal 5(1), 1-23.*

Srikhirin, P., Aphornratana, S., & Chungpaibulpatana, S. (2001). A review of absorption refrigeration technologies. *Renewable and*

sustainable energy reviews, 5(4), 343-372.

Thumann, A., & Mehta, D. P. (2001). *Handbook of energy engineering*: The Fairmont Press, Inc.

Wang, X., & Chua, H. T. (2009). Absorption cooling: a review of lithium bromide-water chiller technologies. *Recent Patents on Mechanical Engineering, 2*(3), 193-213.

Winston, R., Jiang, L., & Widyolar, B. (2014). Performance of a 23KW solar thermal cooling system employing a double effect absorption chiller and thermodynamically efficient non-

tracking concentrators. *Energy Procedia, 48*, 1036-1046.

Wu, D., & Wang, R. (2006). Combined cooling, heating and power: a review. *progress in energy and combustion science, 32*(5-6), 459-495.

Xu, G., & Dai, Y. (1997). Theoretical analysis and optimization of a double-effect parallel-flow-type absorption chiller. *Applied thermal engineering, 17*(2), 157-170.

Xu, G., Dai, Y., Tou, K., & Tso, C. (1996). Theoretical analysis and optimization of a double-effect series-flow-type absorption chiller. *Applied thermal engineering, 16*(12), 975-987.